CHAPTER IV

RESULTS AND DISCUSSION

4.1 Characteristics of Catalysts

In this study, four types of catalysts, namely Ag/(LSA)α-Al_2O_3, Ag/(HSA)α-Al_2O_3, Au-Ag/(HSA)α-Al_2O_3, and Au/TiO_2, were used for investigating the ethylene epoxidation activity in the combined catalyst and low-temperature corona discharge system. The measured values of the actual metal loading content and the BET surface areas of all the studied catalysts are shown comparatively in Table 4.1. The actual metal loading content of these four catalysts obtained from AAS was not significantly different from the nominal metal loading content. This implies that the incipient wetness impregnation technique used for loading metals on different supports is reliably effective, resulting in no significant loss of metals during the preparation.

The BET surface areas of the Ag/(LSA)α-Al_2O_3 family slightly increased with increasing silver loading content, indicating that the silver particles were well dispersed on the support without the sintering effect. The surface area of these well-dispersed Ag particles, despite small amount as compared to the support, attributed to the increase in the surface area of the catalysts with extremely low surface area support.

For other catalysts, their surface areas were similar to those of the unloaded supports in the range of 98-101 m^2/g for the (HSA)α-Al_2O_3 support and 59-61 m^2/g for the TiO_2 support. These results imply that both Ag and/or Au were dispersed on the surface of both high surface area supports (Rojluechai *et al.,* 2006).

The XRD patterns of all the studied catalysts are shown in Figure 4.1–4.3. For the 1 wt% Au/TiO_2 catalyst in Figure 4.1, both the anatase and rutile peaks were observed in this sample, while the presence of small peaks responsible for gold was also observed. For the (HSA)α-Al_2O_3 series in Figure 4.2, the presence of Au does not alter the typical XRD pattern of the Ag catalyst, giving obvious tailing at about

38, 44, and 64° (2θ) and also suggesting that Au was highly dispersed on bimetallic catalyst.

Table 4.1 Textural characteristics of all prepared catalysts

Catalyst	Nominal content (wt%)		Actual Ag content[a] (wt%)	Actual Au content[a] (wt%)	BET surface area (m^2/g)
	Ag	Au			
$Ag/(LSA)\alpha\text{-}Al_2O_3$	0	0	0	0	0.44
	10	0	9.63	0	0.61
	12.5	0	12.54	0	0.74
	15	0	14.94	0	0.89
$Ag/(HSA)\alpha\text{-}Al_2O_3$	0	0	0	0	101
	13.18	0	12.98	0	98
$Au\text{-}Ag/(HSA)\alpha\text{-}Al_2O_3$	13.18	0.63	12.98	0.78	97
Au/TiO_2	0	0	0	0	61
	0	1	0	0.93	59

[a] Results obtained from AAS

Figure 4.3 illustrates the XRD patterns of Ag catalyst on low surface area alumina at different silver loading content. For the unloaded support, only $\alpha\text{-}Al_2O_3$ phase was observed as a major phase. The silver phase was found when silver loading increased up to 15 wt% Ag. At 15 wt% Ag, silver nitrate phase was observed probably due to overloading of Ag precursor.

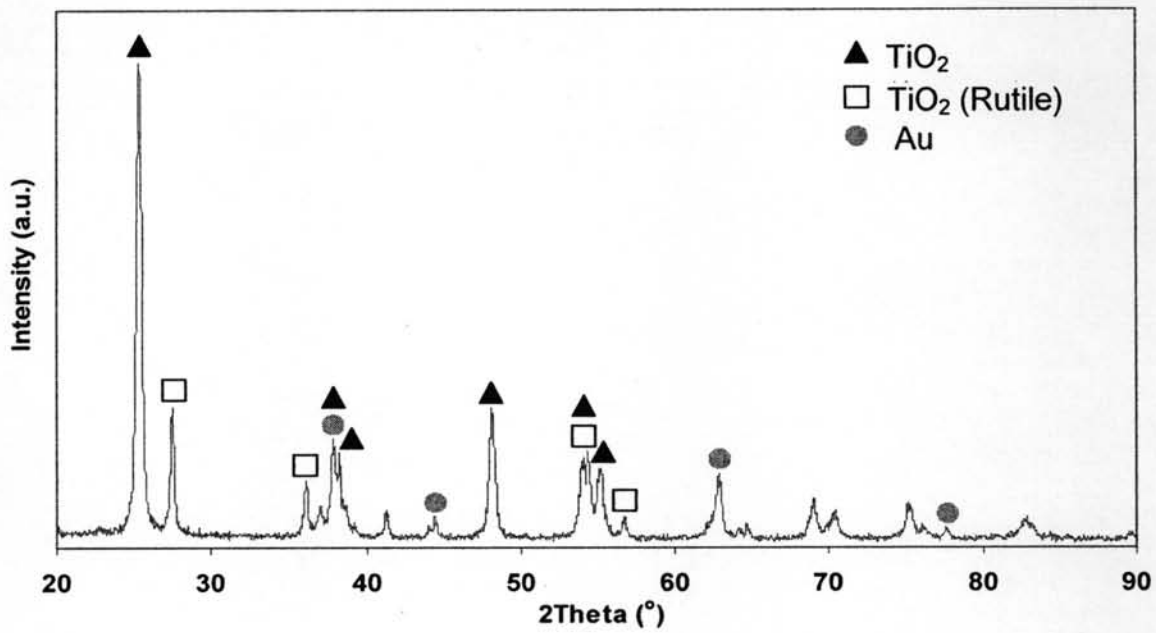

Figure 4.1 XRD pattern of 1 wt% Au/TiO_2 catalyst.

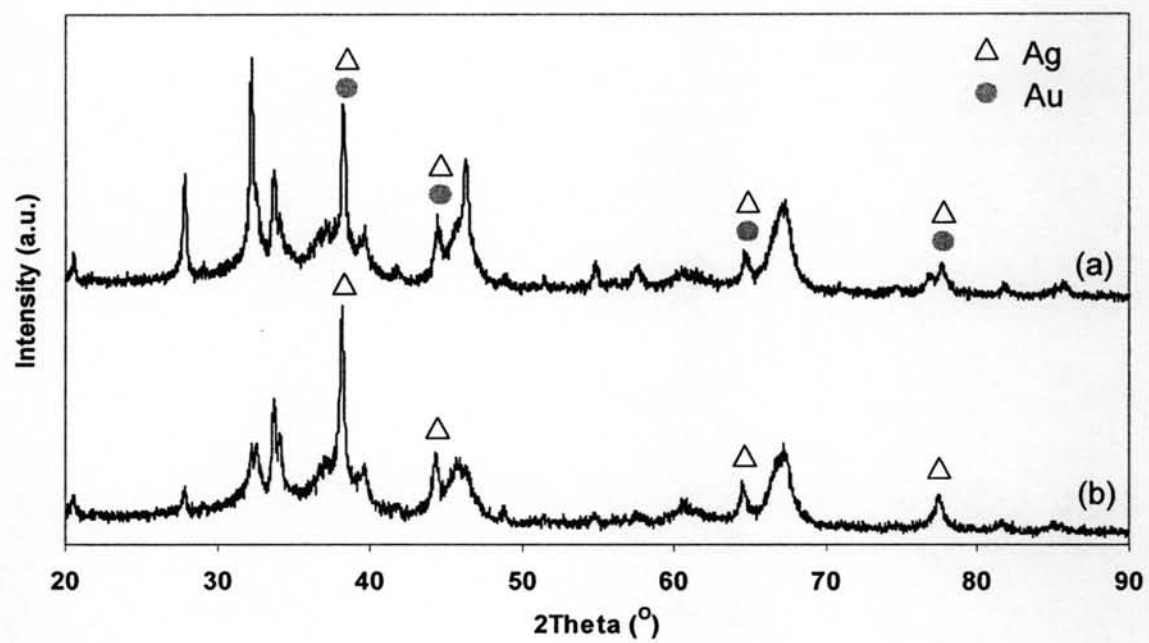

Figure 4.2 XRD patterns of (a) 13.18 wt% Ag/(HSA)α-Al_2O_3 and (b) 0.63 wt% Au-13.18 wt% Ag/(HSA)α-Al_2O_3, respectively.

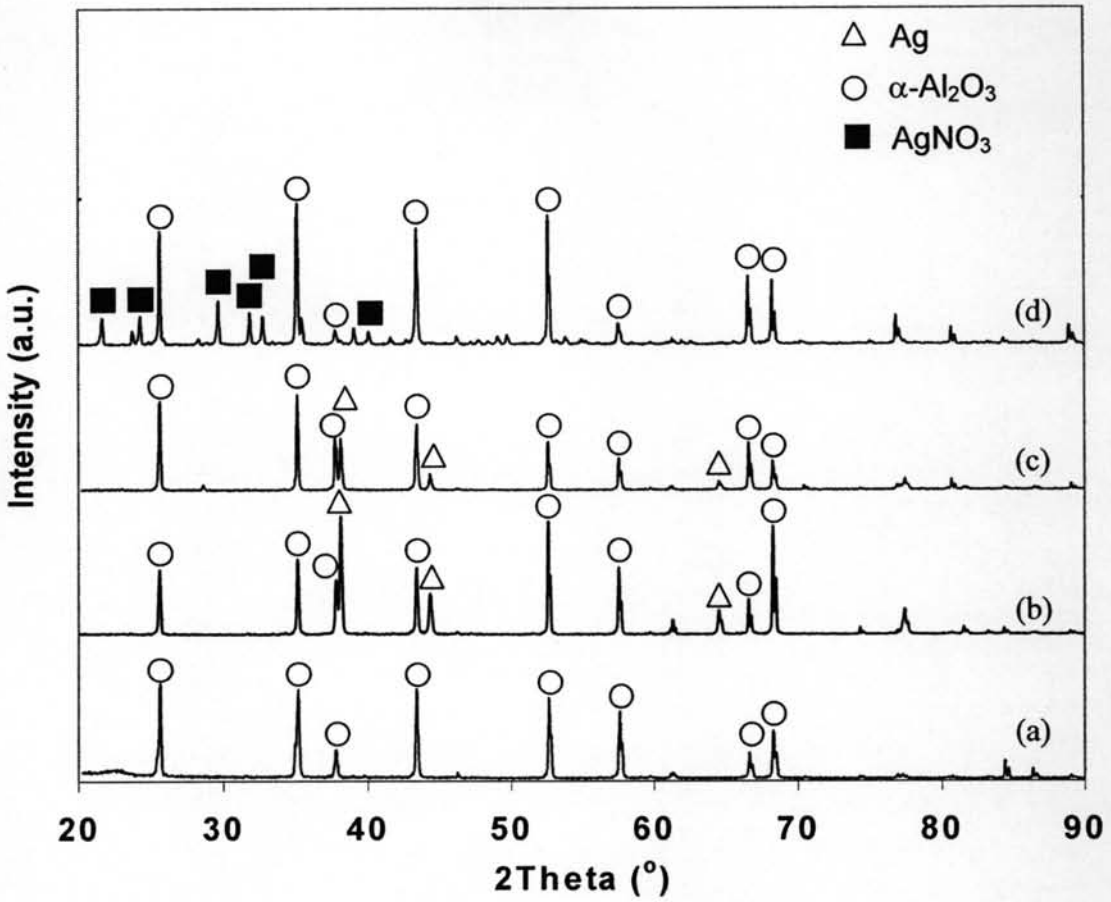

Figure 4.3 XRD patterns of (a) (LSA)α-Al_2O_3, (b) 10 wt% Ag/(LSA) α-Al_2O_3, (c) 12.5 wt% Ag/(LSA)α-Al_2O_3, and (d) 15 wt% Ag/(LSA)α-Al_2O_3, respectively.

In this study, TEM was employed to observe the morphology and mean particle size of Ag on the surface of the studied catalysis. The results from the TEM analysis show that Ag particles are highly dispersed on the alumina support, as depicted in Figure 4.4. TEM micrographs of representative 12.5 wt% Ag/(LSA)α-Al_2O_3, which exhibited the superior activity toward the ethylene epoxidation as explained later, revealed mean Ag particle size of approximately 9.4 nm, as shown in Figure 4.5.

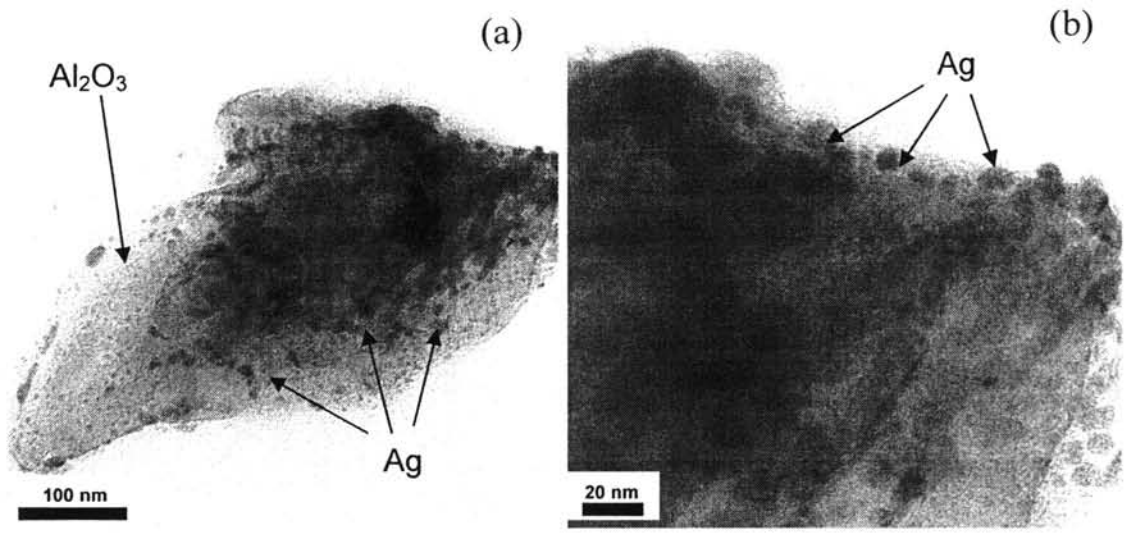

Figure 4.4 TEM images of 12.5 wt% Ag/(LSA)α-Al_2O_3 at (a) low magnification and (b) high magnification.

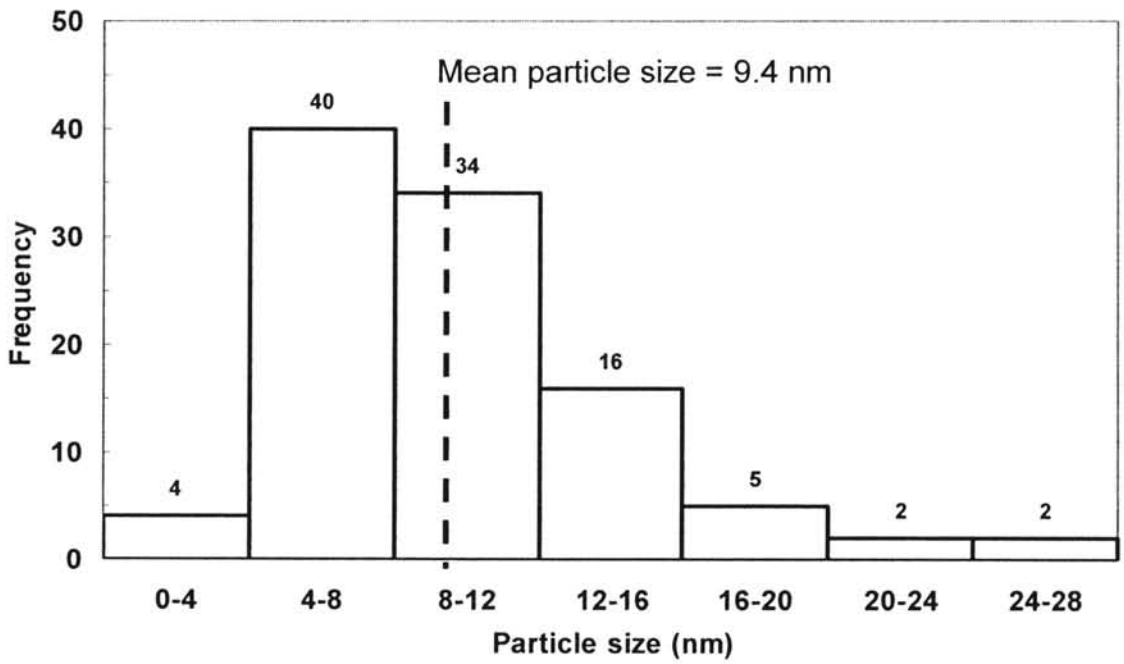

Figure 4.5 Histogram of Ag particle size distribution for 12.5 wt% Ag/(LSA)α-Al_2O_3 determined by TEM.

4.2 Reaction Activity Performance

4.2.1 Effect of Type of Catalysts

As mentioned above, a comparison of ethylene epoxidation in the absence and the presence of different catalysts under the low-temperature corona discharge were initially studied in order to obtain the most suitable catalyst providing the best ethylene oxide selectivity. All experiments were carried out at ambient temperature and atmospheric pressure. The products from the reaction were carbon dioxide, carbon monoxide, ethylene oxide, ac etylene, methane, small amount of ethane, and traces of C_3–C_4.

4.2.1.1 Effect of Type of Catalysts on Ethylene and Oxygen Conversions and Product Selectivities

In the reactor with an empty discharge gap, gas phase reactions induced by discharge mainly contribute to the reactant conversions. In corona discharge system, most of discharge energy is used to produce and accelerate electrons, which then react with gas molecules to generate highly active species (metastables, radicals, and ions). Ethylene and oxygen are therefore chemically activated directly by electron collisions. For combined catalytic-plasma system, catalytic material in the plasma or discharge zone is used to improve the selectivity and efficiency of plasma process by surface reactions.

Figures 4. 7 and 4.8 show the conversions of ethylene and oxygen and the product selectivities over different catalysts, respectively. It was found that ethylene conversion was less than oxygen conversion in both sole plasma and combined catalytic-plasma system since the bond dissociation energy of ethylene (682 kJ/mol) is much more than that of oxygen (498.38 kJ/mol). In sole plasma system, it provided the highest oxygen conversion. Oxygen conversion on Ag/(HSA)α-Al_2O_3 was higher than that on Ag/(LSA)α-Al_2O_3 since the high surface area alumina support could provide higher silver dispersion than the low surface area one, therefore improving oxygen adsorption for the oxidation reaction to result in higher oxygen conversion.

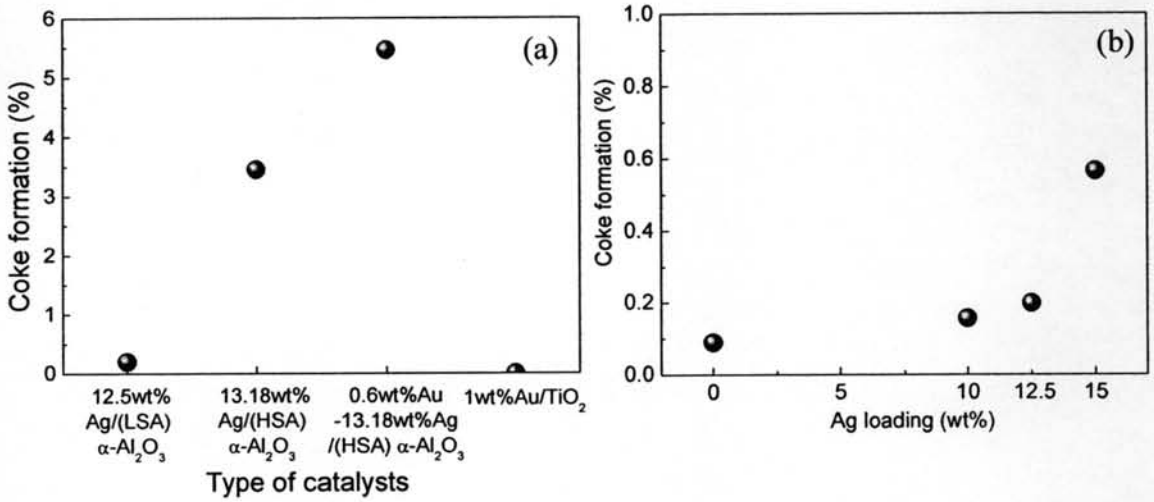

Figure 4.6 Coke formation on spent catalysts determined by TPO: (a) different catalysts and (b) different silver loadings on (LSA)α-Al_2O_3.

After the reaction occurred, the coke formation on different spent catalysts was investigated by TPO, as depicted in Figure 4.6. It is found that the amounts of coke formed were approximately 0.20, 3.45, and 5.46% of total catalyst weight, respectively, for Ag/(LSA)α-Al_2O_3, Ag/(HSA)α-Al_2O_3, and Au-Ag/(HSA)α-Al_2O_3, while the coke deposit did not occur on the Au/TiO_2 catalyst, as shown in Figure 4.6(a), due to its extremely low activity. For the spent Ag/(LSA)α-Al_2O_3 catalyst, which exhibited the highest activity among all investigated catalysts, it can be observed that the coke formation increased as a function of Ag loading content on (LSA)α-Al_2O_3, especially at Ag loading content higher than 12.5 wt%, as shown the Figure 4.6(b).

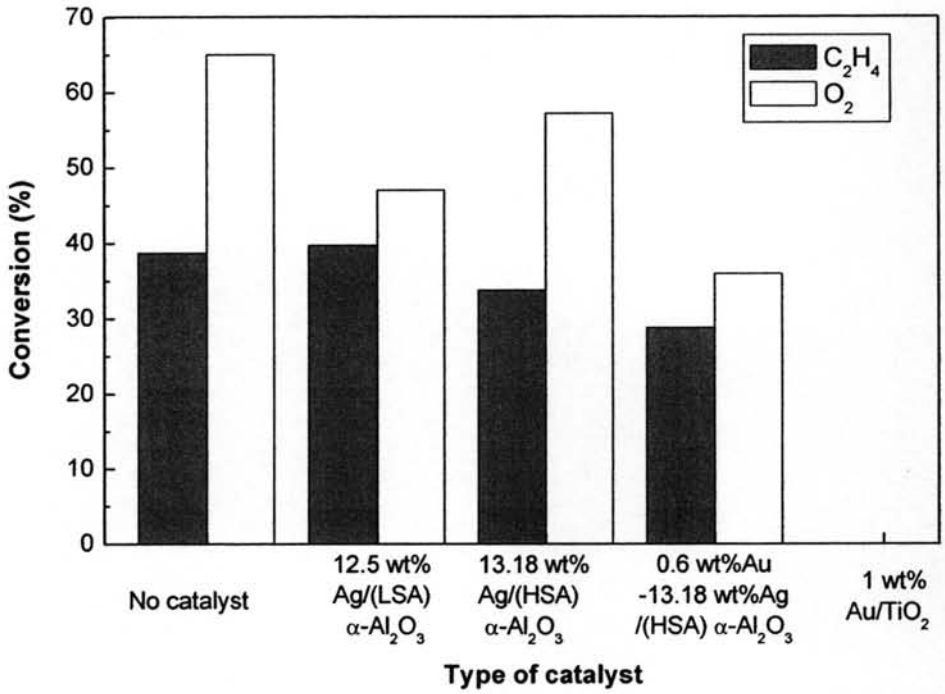

Figure 4.7 Conversions of ethylene and oxygen over different catalysts (molar ratio of O_2/C_2H_4 = 1/1; total feed flow rate = 50 mL/min; gap distance = 1 cm; frequency = 500 Hz; and voltage = 15 kV).

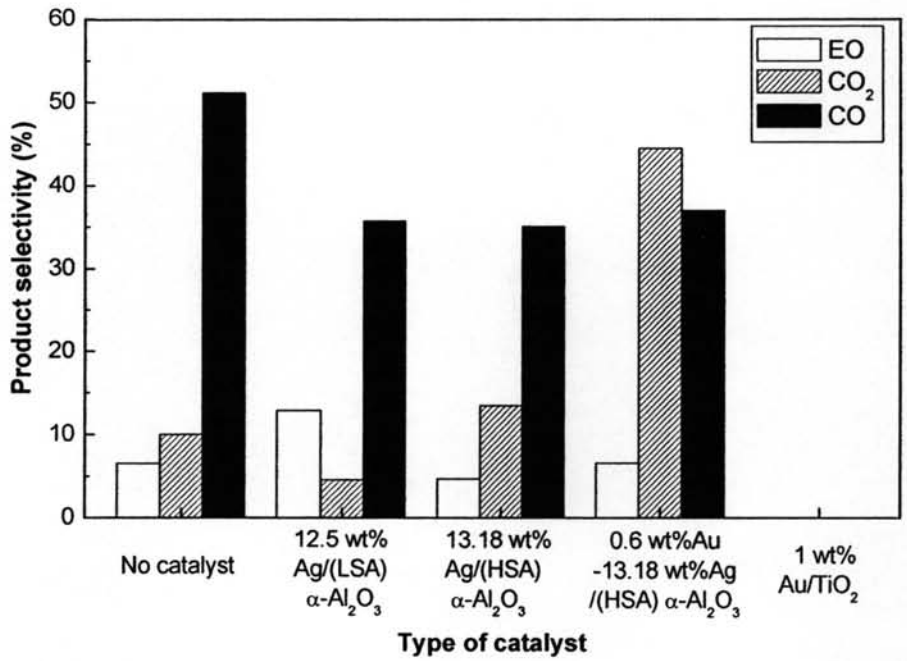

Figure 4.8 Product selectivities over different catalysts (molar ratio of O_2/C_2H_4 = 1/1; total feed flow rate = 50 mL/min; gap distance = 1 cm; frequency = 500 Hz; and voltage = 15 kV).

For bimetallic Au-Ag/(HSA)α-Al_2O_3, it was found to give a lower oxygen conversion than both Ag/(HSA)α-Al_2O_3 and Ag/(LSA)α-Al_2O_3. The explanation is that if chemisorption-induced surface enrichment was operative, it would tend to enhance the concentration of Ag on the surface, not reduce it. This is due to the fact that oxygen forms strong chemisorption bonds with silver, while it does not adsorb, at any appreciable extent, on gold. It is well known that the component, which forms the strongest chemisorption bonds, tends to segregate at the surface of the alloy particles. The alloys in this study were exposed to oxygen during preparation (Geenen *et al.*, 1982). Interestingly, higher ethylene and oxygen conversions induced by plasma system were higher than those in the case of combined catalyst and plasma system. This result indicates that the activity of plasma can be slightly retarded in the presence of catalyst since catalyst reduces the volume of plasma zone, as well as acts as an electrically resistant material.

By considering the product selectivities, it can be seen that type of catalysts significantly affected to the selectivities of main products, i.e. C_2H_4O, CO, and CO_2. Even though bimetallic Au-Ag/(HSA)α-Al_2O_3 combined with plasma was shown to favor the total oxidation reaction as compared to other catalysts, it still provided a moderate ethylene oxide selectivity, even higher as compared to Ag/(HSA)α-Al_2O_3. The reason is that gold could behave as a diluting agent on silver surface, resulting in destroying multiple silver sites which favor atomic oxygen adsorption. As a result, addition of gold simply creates new adsorption sites for molecular oxygen, which is also responsible for the ethylene epoxidation reaction (Rojluechai *et al.*, 2006). However, the reason for the highest selectivity of carbon dioxide is attributed to the O^{2-} species that are separated from one another, and the adsorbed ethylene complex that can consequently react with atomic oxygen to form carbon dioxide and water (Geenen *et al.*, 1982). Clearly, Ag/(HSA)α-Al_2O_3 catalysts were found to be more active for total oxidation reaction than Ag/(LSA)α-Al_2O_3 and sole plasma system. In plasma system, it was found to show the highest selectivity of carbon monoxide and a low selectivity of carbon dioxide, while no reaction occurred in the system with Au/TiO_2 catalyst.

It is generally accepted that the cold plasma changes the status of reactant molecules. Instead of neutral ground state molecules, a mixture of electrons, excited molecules, ions, and radicals occupies in the plasma zone. The energized electrons and excited active species are in a thermodynamically initial state for subsequent reactions. Besides, the interactions among the active species and catalyst lead to an unusual plasma catalytic reaction (Malik *et al.*, 2006).

To obtain a better understanding of the ethylene epoxidation reactions in plasma environment, it is worth describing all the possibilities of chemical pathways for plasmas to activate oxygen molecules, as shown in the following reactions (Liu *et al.*, 1996):

Dissociation attachment:

$$e^- + O_2 \rightarrow O^- + O \quad (4.1)$$

Attachment:

$$e^- + O_2 \rightarrow O_2^- \quad (4.2)$$

Dissociation:

$$e^- + O_2 \rightarrow 2O + e^- \quad (4.3)$$

In general, methyl radical formation is a major important role in radical reaction intiation, leading to higher hydrocarbon production. The principal products generated by subsequent reactions are as follows (Liu *et al.*, 1998):

Ethane formation:

$$CH_3 + CH_3 \rightarrow C_2H_6 \quad (4.4)$$

$$CH_4 + CH_2 \rightarrow C_2H_6 \quad (4.5)$$

$$C_2H_6 + H \rightarrow C_2H_5 + H_2 \quad (4.6)$$

$$C_2H_5 + C_2H_5 \rightarrow C_2H_6 + C_2H_4 \quad (4.7)$$

Ethylene formation:

$$C_2H_6 \rightarrow C_2H_4 + H_2 \quad (4.8)$$

$$C_2H_6 \rightarrow CH_3 + CH_3 \quad (4.9)$$

$$CH_3 + CH_3 \rightarrow C_2H_4 + H_2 \quad (4.10)$$

$$CH_3 + CH_2 \rightarrow C_2H_4 + H \quad (4.11)$$

$$CH_2 + CH_2 \rightarrow C_2H_4 \quad (4.12)$$

$$CH_3 + CH_3 \rightarrow C_2H_5 + H \quad (4.13)$$

$$C_2H_6 + H \rightarrow C_2H_5 + H_2 \quad (4.14)$$

$$C_2H_6 + CH_3 \rightarrow CH_4 + C_2H_5 \quad (4.15)$$

$$C_2H_5 + H \rightarrow CH_3 + CH_3 \quad (4.16)$$

$$C_2H_5 + H \rightarrow C_2H_4 + H_2 \quad (4.17)$$

Acetylene formation:

$$C_2H_4 \rightarrow C_2H_2 + H_2 \quad (4.18)$$

$$CH_2 + CH_2 \rightarrow C_2H_2 + H_2 \quad (4.19)$$

$$C_2H_4 + H \rightarrow C_2H_3 + H_2 \quad (4.20)$$

$$C_2H_3 + H \rightarrow C_2H_2 + H_2 \quad (4.21)$$

$$CH + CH \rightarrow C_2H_2 \quad (4.22)$$

$$CH_2 + CH \rightarrow C_2H_2 + H \quad (4.23)$$

Carbon oxide (CO_x) formation:

$$CH_3 + O \rightarrow HCHO + H \quad (4.24)$$

$$HCHO + O \rightarrow OH + CHO \quad (4.25)$$

$$CHO + O \rightarrow OH + CO \quad (4.26)$$

$$CHO + O \rightarrow CO_2 + H \quad (4.27)$$

$$HCHO + H \rightarrow H_2 + CHO \quad (4.28)$$

$$CHO + H \rightarrow H_2 + CO \quad (4.29)$$

$$HCHO + OH \rightarrow CHO + H_2O \quad (4.30)$$

$$CHO + OH \rightarrow CO + H_2O \quad (4.31)$$

$$C_2H_4 + 3O_2 \rightarrow 2CO_2 + 2H_2O \quad (4.32)$$

$$C_2H_4O + 5/2O_2 \rightarrow CO_2 + H_2O \quad (4.33)$$

Ethylene oxide (EO) formation:

$$C_2H_4 + O \rightarrow C_2H_4O \quad (4.34)$$

$$C_2H_6 + O \rightarrow C_2H_4O + H_2 \quad (4.35)$$

$$C_2H_5 + O \rightarrow C_2H_4O + H \quad (4.36)$$

Other reactions:

$$C_2H_4 + O \rightarrow C_2H_3 + OH \quad (4.37)$$

$$C_2H_3 + 4O \rightarrow 2CO_2 + 3H \quad (4.38)$$

$$C_2H_3 + O \rightarrow C_2H_2 + OH \quad (4.39)$$

$$C_2H_2 + 5O \rightarrow 2CO_2 + H_2O \quad (4.40)$$

$$C_2H_2 + O \rightarrow C_2H_2O \quad (4.41)$$

$$C_2H_2O + 4O \rightarrow 2CO_2 + H_2O \quad (4.42)$$

$$C_2H_2O + O \rightarrow 2CHO \quad (4.43)$$

$$2CHO + O \rightarrow H_2 + 2CO_2 \quad (4.44)$$

$$H_2 + O \rightarrow H_2O \quad (4.45)$$

$$CO + O \rightarrow CO_2 \quad (4.46)$$

In comparison, among these four catalysts combined with plasma system and sole plasma system, it is clear that the presence of suitable catalyst in corona discharge can enhance the selectivity of the desired product, ethylene oxide. In this experimental part, Ag/(LSA)α-Al_2O_3 catalyst was found to offer the highest selectivity of ethylene oxide and the lowest selectivities of carbon dioxide and carbon monoxide. In addition, the coke formed on spent Ag/(LSA)α-Al_2O_3 was comparatively low, as shown in Figure 4.6(a). Hence, Ag/(LSA)α-Al_2O_3 catalyst was selected for further studies.

4.2.2 Effect of Silver Loading Content

Due to the superior activity toward ethylene epoxidation of Ag/(LSA)α-Al_2O_3 catalyst, the silver loading content on this catalyst was varied in the range of 0 to 15 wt%, while input frequency, applied voltage, feed flow rate, and O_2/C_2H_4 molar ratio were kept constant in order to determine the effect of silver

loading. The plasma system with (LSA)α-Al_2O_3 catalyst loaded with Ag content of higher 20 wt% could not be operated until reaching steady state due to high amount of coke formation between the pin electrode and the surface of catalyst.

4.2.2.1 Effect of Silver Loading Content on Ethylene and Oxygen Conversions and Product Selectivities

Figure 4.9 illustrates the conversions of C_2H_4 and O_2 and the products selectivities over Ag/(LSA)α-Al_2O_3 as a function of silver loading content. It was found that the lowest ethylene and oxygen conversions were observed for the blank support, as compared to the Ag-loaded ones. This result indicates that the presence of silver loading on this support is necessarily important to enhance both C_2H_4 and O_2 conversions. The conversion of C_2H_4 increased with increasing Ag loading to 10 wt% and remained almost constant up to 15 wt% Ag, while the conversion of O_2 also increased with increasing Ag loading to 10 wt% but substantially decreased with further increasing the loading content. At high Ag loading content, especially higher than 12.5 wt%, the amount of coke formed was relatively high as shown in Figure 4.6(b), resulting in the negative activity with low O_2 conversion.

The influence of silver loading content on the selectivities of C_2H_4O, CO, and CO_2 is depicted in Figure 4.9. It is apparent that an increase in silver loading content resulted in an increase in both CO and CO_2 selectivities, especially with Ag loading content higher than 12.5 wt%, however the selectivities of C_2H_4O increased up to 12.5 wt% Ag and substantially declined with further increasing Ag loading content. Table 4.2 also shows that the selectivities of C_2H_2 and C_3H_6 tended to decrease as silver loading content increased, whereas the selectivities of CH_4 and C_2H_6 remained almost unchanged. By considering the activity of the catalyst with various Ag loading content in terms of product selectivity, 12.5 wt% Ag was very suitable for the reaction because it provided relatively high C_2H_4O selectivity and low CO and CO_2 selectivities.

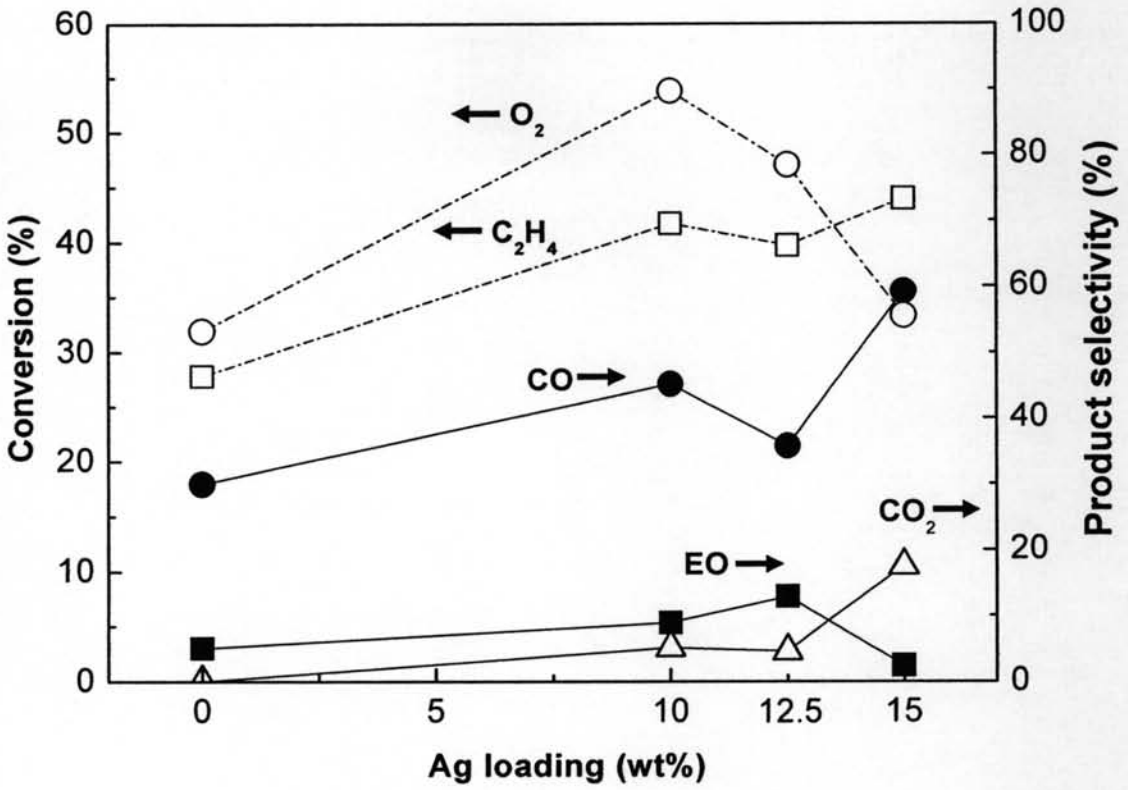

Figure 4.9 Conversions of ethylene and oxygen and product selectivities as a function of Ag loading content on (LSA)α-Al_2O_3 (molar ratio of O_2/C_2H_4 = 1/1; feed flow rate = 50 mL/min; gap distance = 1 cm; frequency = 500 Hz; and voltage = 15 kV).

Table 4.2 By-product selectivities as a function of Ag loading content on (LSA)α-Al_2O_3 (molar ratio of O_2/C_2H_4 = 1/1; feed flow rate = 50 mL/min; gap distance = 1 cm; frequency = 500 Hz; and voltage = 15 kV)

Silver loading content (wt%)	By-product selectivity (%)			
	CH_4	C_2H_2	C_2H_6	C_3H_6
0	2.95	25.99	4.67	5.72
10	4.97	19.77	7.09	5.28
12.5	4.22	17.28	6.12	3.01
15	4.84	9.77	4.49	2.10

4.2.2.2 Comparison of Specific Energy Consumption for Different Silver Loadings

Figure 4.10 shows the effect of silver loading content on the power consumption. With increasing silver loading, the power consumption per molecule of C_2H_4 converted or per molecule of C_2H_4O produced substantially decreased up to 12.5 wt% Ag. At higher silver loading, the power consumption dramatically increased. The result indicates that the lowest power consumption for converting ethylene molecule to produce ethylene oxide molecule can be attained when the silver loading is 12.5 wt%. The 12.5 wt% Ag/(LSA)α-Al_2O_3 was selected for further experiments since it gave high conversions of ethylene and oxygen, high selectivity of ethylene oxide, as well as low power consumption.

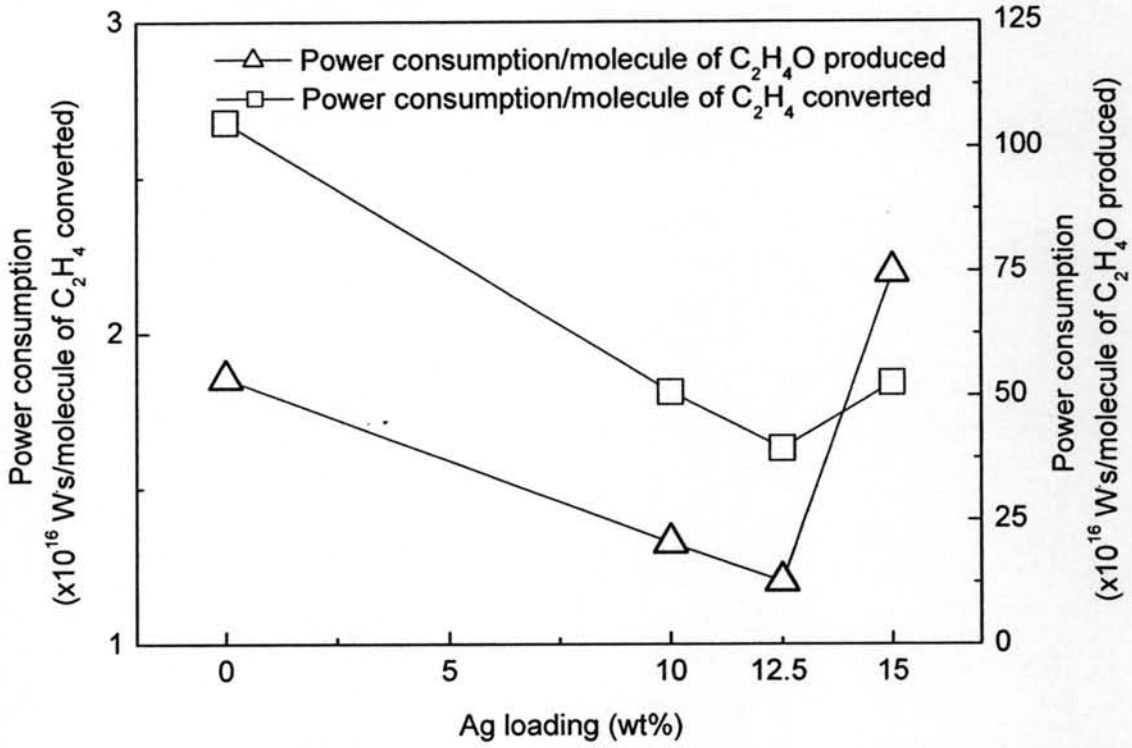

Figure 4.10 Comparison of specific energy consumption for different silver loadings on (LSA)α-Al_2O_3 (molar ratio of O_2/C_2H_4 = 1/1; feed flow rate = 50 mL/min; gap distance = 1 cm; frequency = 500 Hz; and voltage = 15 kV).

4.2.3 Effect of Applied Voltage

From the preliminary tests on the voltage range that could be applied to the system, the break-down voltage or the lowest voltage (onset voltage) to generate plasma was found to be about 7 kV, and the plasma system could not be operated at the applied voltage higher than 15 kV since the plasma system could no longer be carried out until reaching steady state due to a large amount of coke formation. Therefore, the reaction experiments were conducted in the voltage range of 7 – 15 kV in order to determine the effect of the applied voltage.

4.2.3.1 Effect of Applied Voltage on Ethylene and Oxygen Conversions and Product Selectivities

The effect of applied voltage on the C_2H_4 and O_2 conversions is illustrated in Figure 4.11. The conversion of oxygen tends to increase with increasing the applied voltage in the range of 7 – 15 kV, whereas the conversion of ethylene remained almost unchanged. The explanation of converted oxygen increment is that a higher voltage results in a higher current, as shown in Figure 4.12, leading to more available electrons that increase an opportunity for collision of oxygen with electrons. Moreover, higher O active species in plasma zone have more opportunity to adsorb on the surface of catalyst for further subsequent reactions. In contrast, it is unexpected that C_2H_4 conversion remained nearly constant with increasing applied voltage. This indicates that the converted C_2H_4 species in plasma zone may be recombined to form C_2H_4 by secondary reaction in the catalytic zone.

The effect of applied voltage on the selectivities of C_2H_4O, CO, CO_2, C_2H_2, CH_4, C_2H_6, and C_3H_6 is shown in Figure 4.11 and Table 4.3. The selectivities of C_2H_4O and CO_2 increased with increasing applied voltage in contrast to the selectivity of C_2H_2, whereas the selectivities of CH_4, C_2H_6, and C_3H_6 remained almost unchanged. When the applied voltage increased corresponding to increasing O active species as mentioned above, active hydrocarbon species are further oxidized to form CO and C_2H_4O on the surface of catalyst, but CO is not further oxidized to CO_2. These results suggest that higher O active species at higher applied voltage is more favorable for C_2H_4O production than complete combustion. Interestingly, certain product from C_2H_4 dehydrogenation in plasma zone, C_2H_2, tended to decrease with increasing the applied voltage due to acetylene hydrogenation on Ag catalyst,

which could be attributed to compensate with the amount of C_2H_4 converted in such the plasma zone and consequently result in unchanged C_2H_4 conversion.

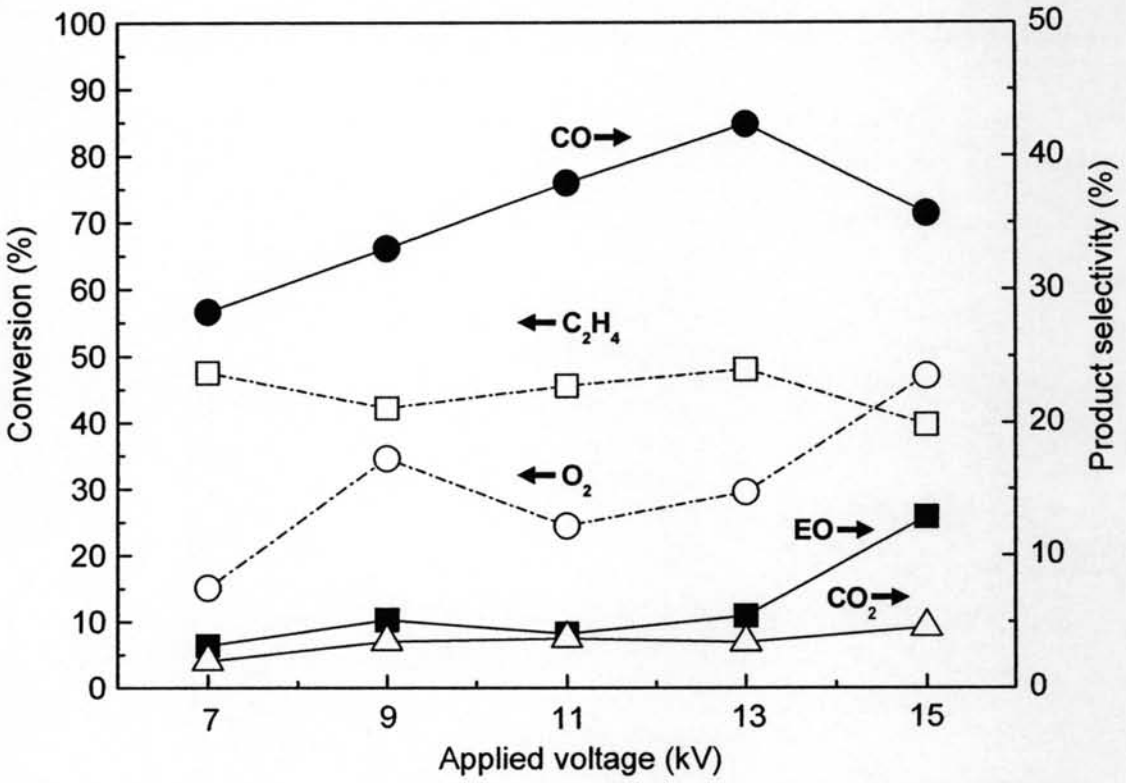

Figure 4.11 Conversions of ethylene and oxygen and product selectivities as a function of applied voltage in the presence of 12.5 wt% Ag on (LSA)α-Al_2O_3 (molar ratio of O_2/C_2H_4 = 1/1; feed flow rate = 50 mL/min; gap distance = 1 cm; and frequency = 500 Hz).

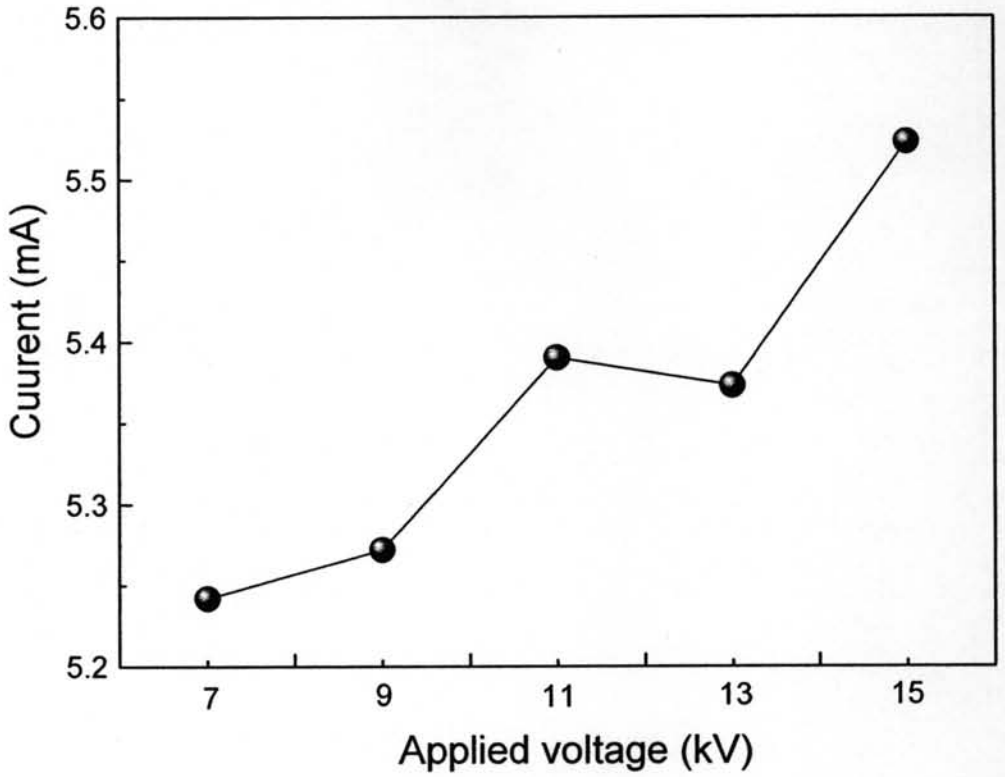

Figure 4.12 Effect of applied voltage on generated current in the presence of 12.5 wt% Ag on (LSA)α-Al_2O_3 (molar ratio of O_2/C_2H_4 = 1/1; feed flow rate = 50 mL/min; gap distance = 1 cm; and frequency = 500 Hz).

Table 4.3 By-product selectivities as a function of applied voltage by using 12.5 wt% Ag on (LSA)α-Al_2O_3 (molar ratio of O_2/C_2H_4 = 1/1; feed flow rate = 50 mL/min; gap distance = 1 cm; and frequency = 500 Hz)

Applied voltage (kV)	By-product selectivity (%)			
	CH_4	C_2H_2	C_2H_6	C_3H_6
7	3.69	21.24	4.55	1.14
9	4.87	28.95	5.65	1.66
11	5.28	19.11	5.37	1.51
13	5.13	14.98	3.36	1.66
15	4.22	17.28	6.12	3.01

4.2.3.2 Comparison of Specific Energy Consumption for Different Applied Voltages

Figure 4.13 shows the effect of applied voltage on the power consumption. With increasing applied voltage, the power consumption per molecule of converted C_2H_4 conversion increased, whereas the power consumption per molecule of produced C_2H_4O substantially decreased. As shown above about the almost unchanged ethylene conversion, the rising average electron energy and the increasing number of electrons in plasma zone could not enhance the conversion of ethylene probably due to C_2H_2 hydrogenation to reform C_2H_4 on the surface of silver catalyst in catalytic zone, resulting in higher energy consumption per molecule of C_2H_4 converted when increasing the applied voltage. In contrast, an increase in the selectivity of C_2H_4O was comparatively high as increasing the applied voltage, resulting in lower power consumption per molecule of produced C_2H_4O. From the results, the optimum voltage of 15 kV, which produced reasonably high conversions of C_2H_4 and O_2 and the highest selectivity of ethylene oxide with the lowest the power consumption per C_2H_4O molecule produced, was selected for further experiments.

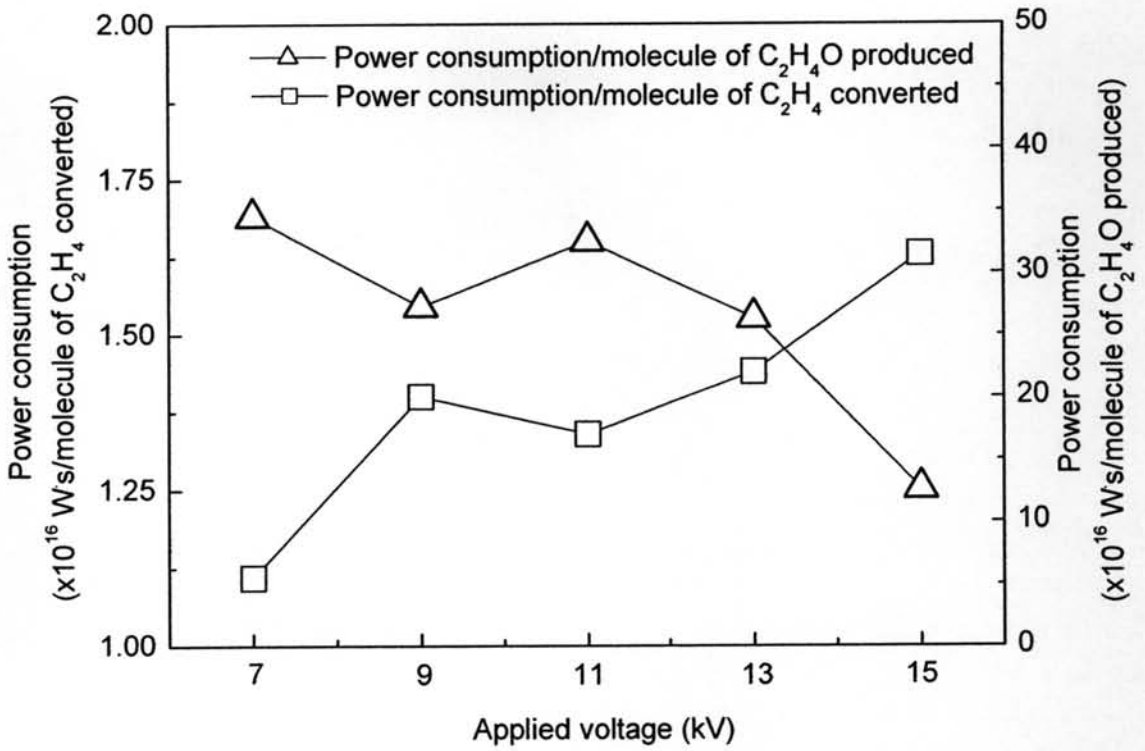

Figure 4.13 Comparison of specific energy consumption for different applied voltages in the presence of 12.5 wt% Ag on (LSA)α-Al_2O_3 (molar ratio of O_2/C_2H_4 = 1/1; feed flow rate = 50 mL/min; gap distance = 1 cm; and frequency = 500 Hz).

4.2.4 Effect of Input Frequency

The studied plasma system was operated in the 300 – 800 Hz frequency range since a large amount of coke was found to deposit on the electrode surface at a frequency lower than 300 Hz, and the plasma could not exist at a frequency higher than 800 Hz.

4.2.4.1 Effect of Input Frequency on Ethylene and Oxygen Conversions and Product Selectivities

The effect of input frequency on the C_2H_4 and O_2 conversions is illustrated in Figure 4.14. When the input frequency increased, the O_2 conversion decreased, whereas C_2H_4 conversion remained almost constant. The explanation is that a higher frequency results in lower current that corresponds to the reduction of the number of electrons generated, as shown in Figure 4.15. Consequently, the opportunity of collision between electrons and O_2 or C_2H_4 molecules declines with decreasing the current. Therefore, it is expected that the conversions of both C_2H_4

and O_2 should decrease with increasing input frequency; however the conversion of C_2H_4 did not follow this expectation. As mentioned before, this is plausibly because of the compensation between C_2H_4 dehydrogenation in plasma zone and C_2H_2 hydrogenation on the surface of silver catalyst in catalytic zone.

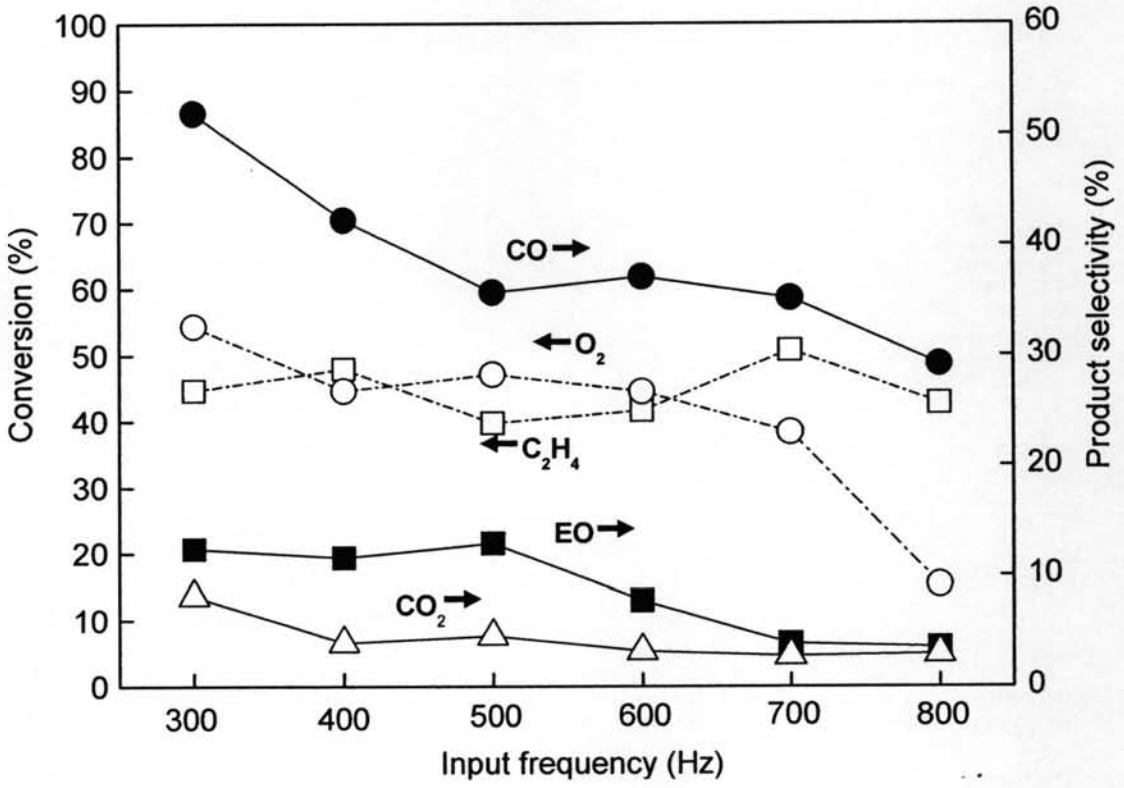

Figure 4.14 Conversions of ethylene and oxygen and product selectivities as a function of input frequency in the presence of 12.5 wt% Ag on (LSA)α-Al_2O_3 (molar ratio of O_2/C_2H_4 = 1/1; feed flow rate = 50 mL/min; gap distance = 1 cm; and applied voltage = 15 kV).

The effect of input frequency on the product selectivities is shown in Figure 4.14 and Table 4.4. The selectivity of C_2H_4O remained nearly unchanged when the frequency was varied in the range of 300-500 Hz. Beyond 500 Hz, the selectivity decreased substantially with increasing frequency. It can be explained that the decrease in the input frequency results in the increased current, as depicted in Figure 4.15. Consequently, there are more O active species available to absorb on the surface of silver catalyst for the epoxidation reaction, leading to the

desired product in the range of 300 to 500 Hz. At higher frequency, the O amount of active species tended to decrease due to less available electron density, resulting in the decrease in the selectivity of C_2H_4O. At the frequency lower than 500 Hz, the selectivity of C_2H_4O did not further increase, despite higher amount of generated electron, because of the coke formation. The selectivities of CO and CO_2 also tended to decrease with increasing input frequency. This is because less O active species at higher input frequency could lead to the decline in the selectivities of CO and CO_2. Therefore, the input frequency of 500 Hz was considered as a potentially optimum condition, exhibiting reasonably high C_2H_4O selectivity with relatively low CO and CO_2 formation.

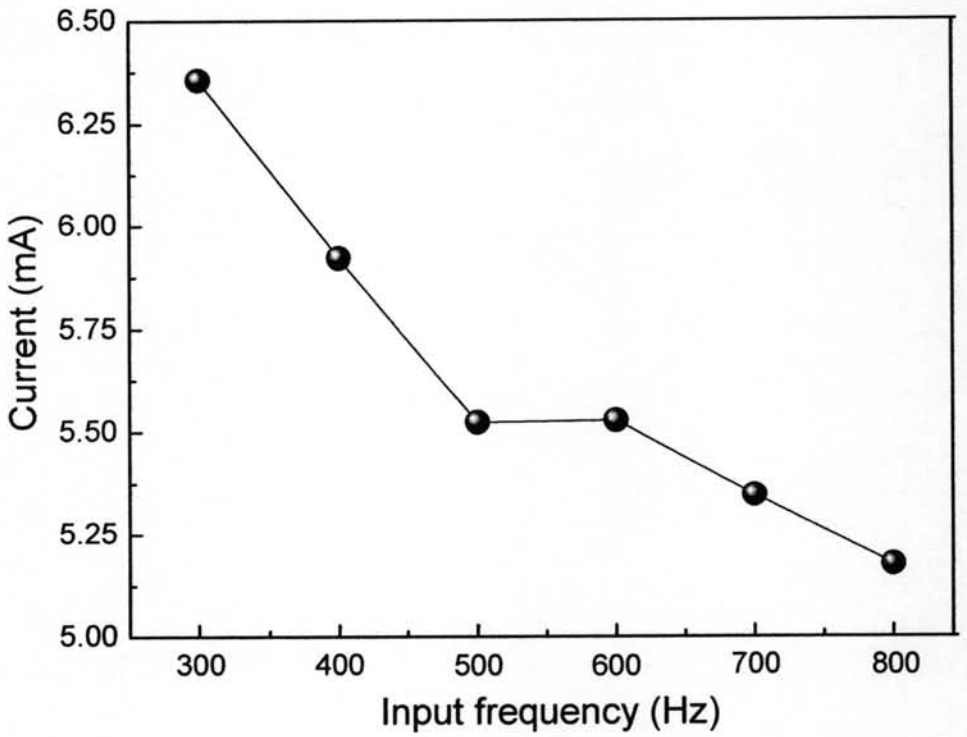

Figure 4.15 Effect of input frequency on generated current in the presence of 12.5 wt% Ag on (LSA)α-Al_2O_3 (molar ratio of O_2/C_2H_4 = 1/1; feed flow rate = 50 mL/min; gap distance = 1 cm; and applied voltage = 15 kV).

Table 4.4 By-product selectivities as a function of input frequency by using 12.5 wt% Ag on (LSA)α-Al_2O_3 (molar ratio of O_2/C_2H_4 = 1/1; feed flow rate = 50 mL/min; gap distance = 1 cm; and applied voltage = 15 kV)

Input frequency (Hz)	By-product selectivity (%)			
	CH_4	C_2H_2	C_2H_6	C_3H_6
300	6.78	14.16	2.51	3.54
400	4.42	13.34	2.96	2.80
500	4.22	17.28	6.12	3.01
600	3.99	17.91	3.53	2.00
700	4.36	15.96	4.14	1.07
800	4.27	21.29	2.89	1.26

4.2.4.2 Comparison of Specific Energy Consumption for Different Input Frequencies

The effect of frequency on the power consumption to break down each C_2H_4 molecule and create each C_2H_4O molecule is shown in Figure 4.16. The result shows that the power consumption per C_2H_4 molecule converted tended to gradually decline as increasing input frequency. While the power consumption to create each C_2H_4O molecule decreased with increasing the input frequency up to 500 Hz, after this frequency, the power consumption dramatically increased. Therefore, the input frequency of 500 Hz can be considered as the optimum value. At a frequency lower than the optimum range, a higher current results in a larger number of electrons, leading to a higher power consumption

Based upon relatively high ethylene oxide selectivity and the lowest power consumption per molecule of ethylene oxide produced, the optimum input frequency of 500 Hz was selected for further experiments. Nevertheless, in this part, coke deposit was observed between the pin electrode and catalyst surface. The amount of coke deposit was found to increase with decreasing frequency, especially at lower than 500 Hz.

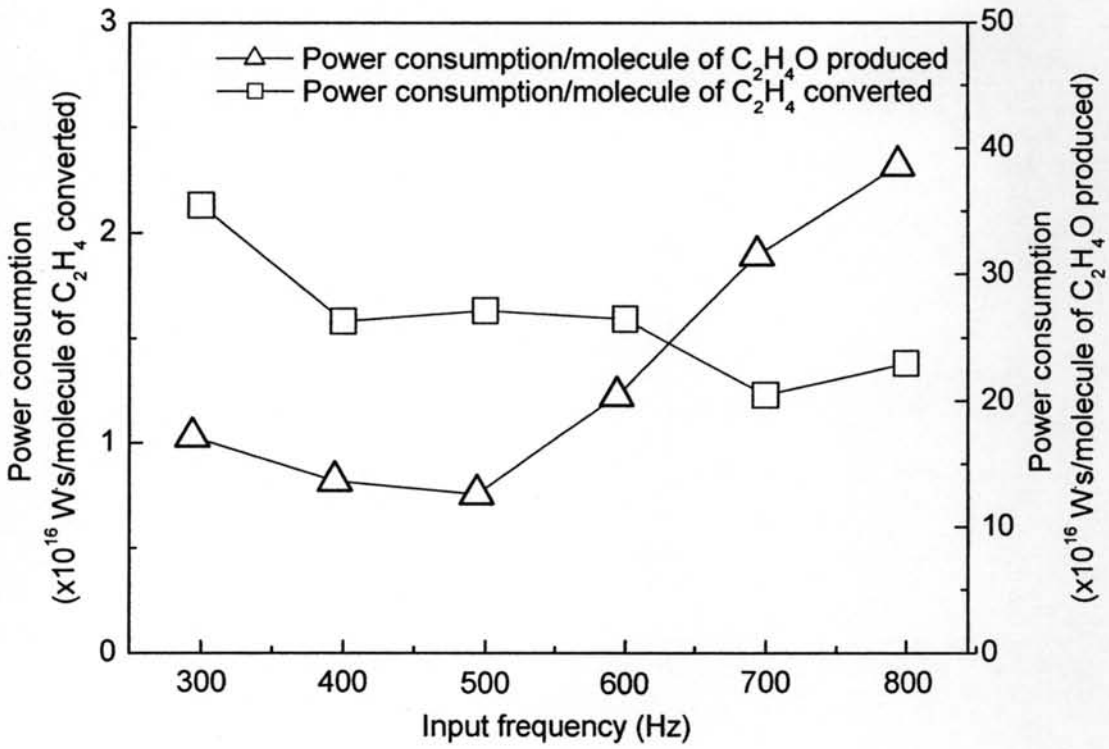

Figure 4.16 Comparison of specific energy consumption for different input frequencies in the presence of 12.5 wt% Ag on (LSA)α-Al_2O_3 (molar ratio of O_2/C_2H_4 = 1/1; feed flow rate = 50 mL/min; gap distance = 1 cm; and applied voltage = 15 kV).

4.2.5 Effect of Molar Ratio of O_2/C_2H_4

To better understand the influence of the feed gas composition on the ethylene epoxidation reaction under corona discharge system, the effect of O_2/C_2H_4 molar ratio was investigated in the range of 1/1 to 5/1. The optimum applied voltage of 15 kV and input frequency of 500 Hz were applied during the reaction.

4.2.5.1 Effect of Molar Ratio of O_2/C_2H_4 on Ethylene and Oxygen Conversions and Product Selectivities

Increasing the O_2/C_2H_4 molar ratio significantly enhanced only the C_2H_4 conversion, while the O_2 conversion also increased at initial stage but tended to decrease with increasing the molar ratio higher than 3/1, as depicted in Figure 4.17. The explanation is that an increase in the molar ratio of O_2/C_2H_4 results in having more O_2 content available to react with ethylene molecules, leading to

higher C_2H_4 conversion. However, the conversion of O_2 reached a maximum at the molar ratio of 3/1, which is the theoretical ratio for C_2H_4 complete combustion as shown in Equation 4.32. At the molar ratio higher than 3/1 or excess O_2 condition, the conversion of O_2 tended to substantially decrease since O_2 was consumed at the same level while initial amount of O_2 was higher.

$$C_2H_4 + 3O_2 \rightarrow 2CO_2 + 2H_2O \qquad (4.32)$$

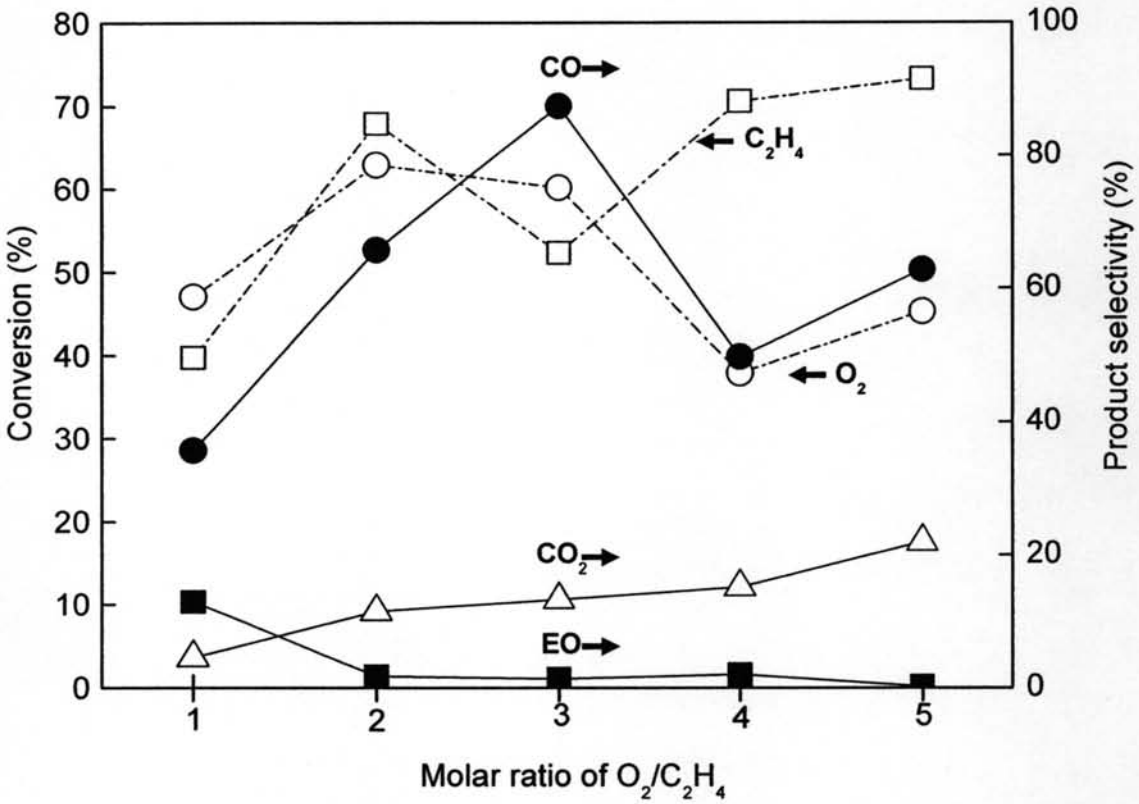

Figure 4.17 Conversions of ethylene and oxygen and product selectivities as a function of O_2/C_2H_4 molar ratio in the presence of 12.5 wt% Ag on (LSA)α-Al_2O_3 (feed flow rate = 50 mL/min; gap distance = 1 cm; applied voltage = 15 kV; and input frequency = 500 Hz).

The effect of O_2/C_2H_4 molar ratio on the selectivities of C_2H_4O, CO, CO_2, C_2H_2, CH_4, C_2H_6, and C_3H_8 is shown as Figure 4.17 and Table 4.5. In this corona discharge system, the selectivities of C_2H_4O, C_2H_2, C_2H_6, and C_3H_6 decreased, but in contrast, the selectivity of CO_2 increased with increasing the O_2/C_2H_4 molar ratio. Interestingly, the selectivities of CO and CH_4 increased up to the O_2/C_2H_4 molar ratio of 3/1, however beyond this value their selectivities rapidly declined. At molar ratio of O_2/C_2H_4 equal to 3/1, O_2 was contributed to form the highest amount of CO. At the molar ratio higher than 3/1, excess O_2 was employed for oxidation of hydrocarbon and CO, resulting in higher amount of CO_2. Moreover, at the O_2/C_2H_4 molar ratio of 5/1, the selectivity of C_2H_4O reached zero level since this molar ratio of O_2/C_2H_4 preferred the complete combustion rather than partial oxidation. This therefore resulted in decreasing hydrocarbon species and increasing CO_2.

Table 4.5 By-product selectivities as a function of O_2/C_2H_4 molar ratio by using 12.5 wt% Ag on (LSA)α-Al_2O_3 (molar ratio of O_2/C_2H_4 = 1/1; feed flow rate = 50 mL/min; gap distance = 1 cm; and applied voltage = 15 kV)

Molar ratio of O_2/C_2H_4	By-product selectivity (%)			
	CH_4	C_2H_2	C_2H_6	C_3H_6
1/1	4.22	17.28	6.12	3.01
2/1	7.12	6.41	4.77	0.97
3/1	10.78	6.73	5.18	0.63
4/1	2.15	1.06	0.94	0.11
5/1	2.28	0.68	0.82	0.10

4.2.5.2 Comparison of Specific Energy Consumption for Different molar ratio of O_2/C_2H_4

Figure 4.18 shows the power consumption to convert ethylene and to produce ethylene oxide molecule at different O_2/C_2H_4 molar ratios. The power consumption per molecule of converted ethylene increased when the O_2/C_2H_4 molar ratio increased up to 3/1. At the O_2/C_2H_4 molar ratio higher than 3/1, the power consumption rapidly decreased. However, there was a significant increase in the power consumption per molecule of produced ethylene oxide with increasing the O_2/C_2H_4 molar ratio, especially at the molar ratio of 5/1. An O_2/C_2H_4 molar ratio of 1/1 was selected for further experiments because it provided the highest selectivity of ethylene oxide and the lowest power consumption, in spite of having the lowest ethylene conversion.

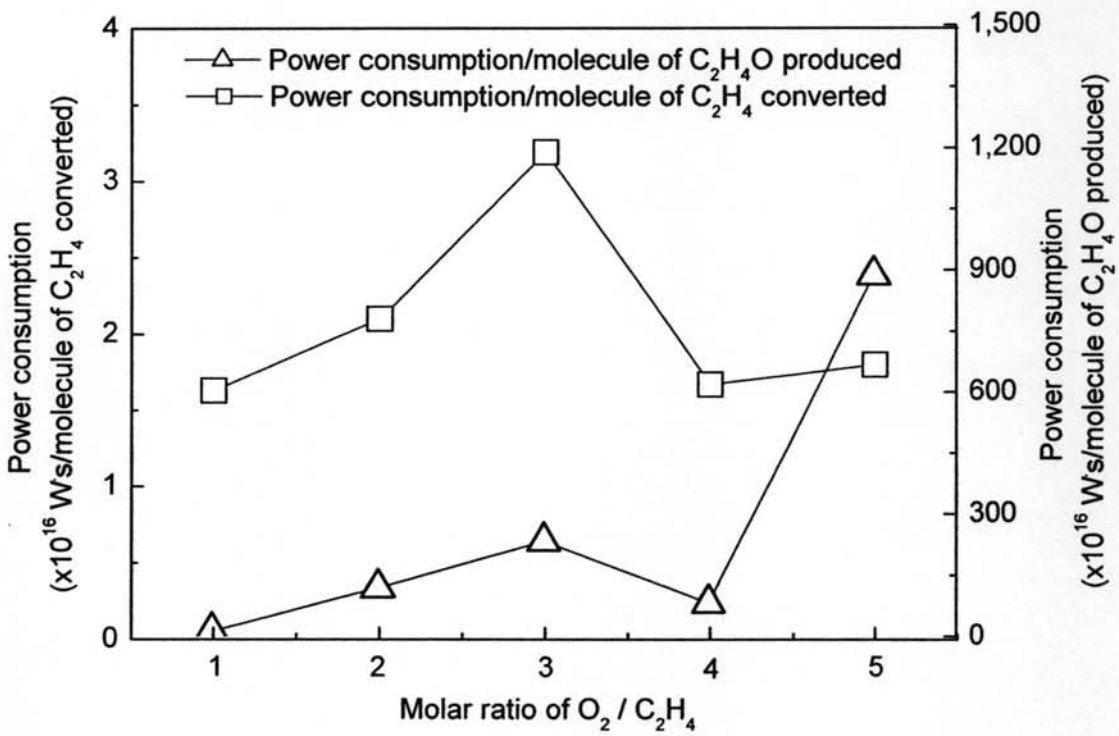

Figure 4.18 Comparison of specific energy consumption for different O_2/C_2H_4 molar ratios in the presence of 12.5 wt% Ag on (LSA)α-Al_2O_3 (feed flow rate = 50 mL/min; gap distance = 1 cm; applied voltage = 15 kV; and input frequency = 500 Hz).

4.2.6 Effects of Feed Flow Rate

The feed flow rate exerts a significant role on the residence time of gas molecules within both plasma and catalytic zones, affecting the performance of the plasma system. The experiments were performed by varying feed flow rate from 50 to 150 mL/min with the O_2/C_2H_4 molar ratio of 1/1. The optimum applied voltage of 15 kV and input frequency of 500 Hz were applied during the reaction.

4.2.6.1 Effect of Feed Flow Rate on Ethylene and Oxygen Conversions and Product Selectivities

Figure 4.19 illustrates the influence of the feed flow rate on the C_2H_4 and O_2 conversions. The conversions of C_2H_4 and O_2 decreased almost linearly with increasing the feed flow rate from 50 to 150 mL/min. An increase in the feed flow rate reduces the gas residence time in the reaction system, resulting in having a shorter contact time of ethylene and oxygen molecules to collide with electrons. As a result, a reduction in the feed flow rate enhanced the conversions of both C_2H_4 and O_2.

The feed flow rate dependence of product selectivities is depicted in Figure 4.19 and Table 4.6. It is apparent that increasing feed flow rate resulted in a decrease in the selectivities of C_2H_4O, CO, CO_2, and other by-products. As above explained, this is because a higher feed flow rate reduces the opportunity of collision between electrons and reactant/intermediate molecules.

4.2.6.2 Comparison of Specific Energy Consumption for Different Feed Flow Rates

Figure 4.20 shows the effect of feed flow rate on the power consumption. Even though the power consumption per molecule of converted ethylene and power consumption per molecule of produced ethylene oxide slightly decreased when increasing feed flow rate, lower feed flow rate gave much higher reactant conversions and desired product selectivity. Therefore, the feed flow rate of 50 mL/min was selected as an optimum value.

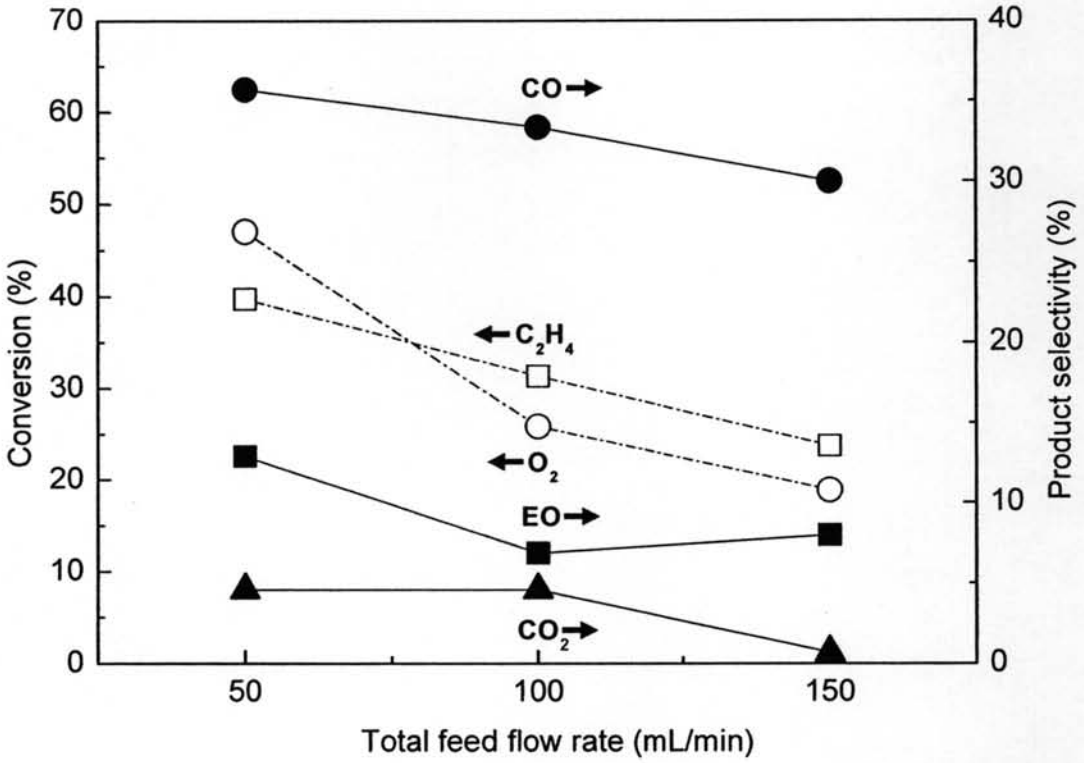

Figure 4.19 Effect of feed flow rate on ethylene and oxygen conversions and product selectivities in the presence of 12.5 wt% Ag on (LSA)α-Al_2O_3 (molar ratio of O_2/C_2H_4 = 1/1; gap distance = 1 cm, applied voltage = 15 kV, and input frequency = 500 Hz).

Table 4.6 By-product selectivities in the presence of 12.5 wt% Ag on (LSA)α-Al_2O_3 (molar ratio of O_2/C_2H_4 = 1/1; gap distance = 1 cm, applied voltage = 15 kV, and input frequency = 500 Hz)

Feed flow rate (mL/min)	By-product selectivity (%)			
	CH_4	C_2H_2	C_2H_6	C_3H_6
50	4.22	17.28	6.12	3.01
100	3.19	15.58	3.40	1.90
150	3.17	18.25	5.17	2.02

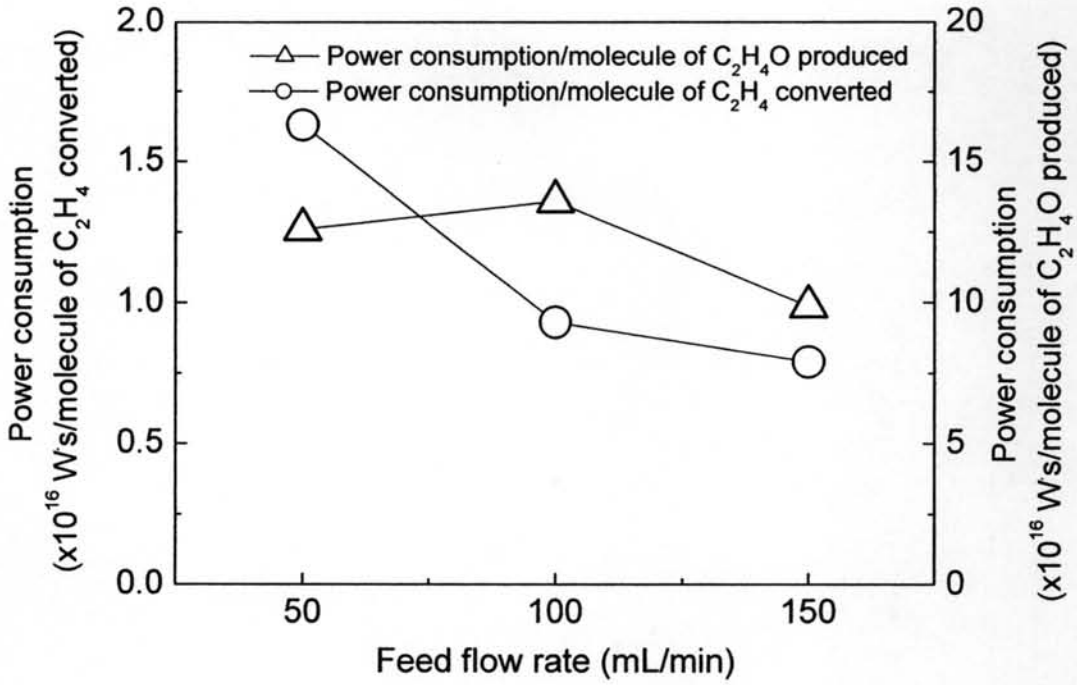

Figure 4.20 Comparison of specific energy consumption for different feed flow rates in the presence of 12.5 wt% Ag on (LSA)α-Al_2O_3 (molar ratio of O_2/C_2H_4 = 1/1; feed flow rate = 50 mL/min; gap distance = 1 cm; applied voltage = 15 kV; and input frequency = 500 Hz).

4.3 Reusability of Catalyst

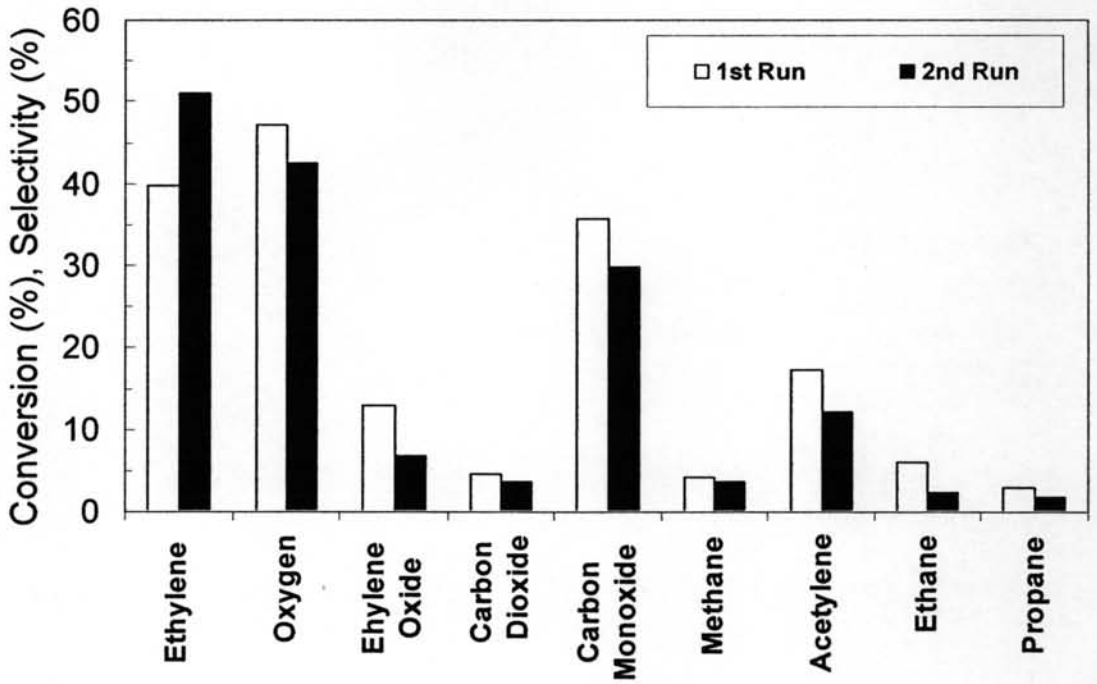

Figure 4.21 The reactant conversions and product selectivity obtained by catalytic-plasma system at the optimum condition for two consecutive runs.

To study the reusability of the spent 12.5 wt% Ag/(LSA)α-Al_2O_3 catalyst, it was taken to perform the activity test in consecutive run without any treatment. Figure 4.21 shows the activity of fresh and spent catalysts in the corona discharge at the optimum condition. This is clear that the activity of spent catalyst was slightly lower than that of fresh catalyst, except the conversion of ethylene.

The explanation is that the lower activity was due to coke formation observed by TPO, as mentioned previously, as well as Ag agglomeration determined by TEM.

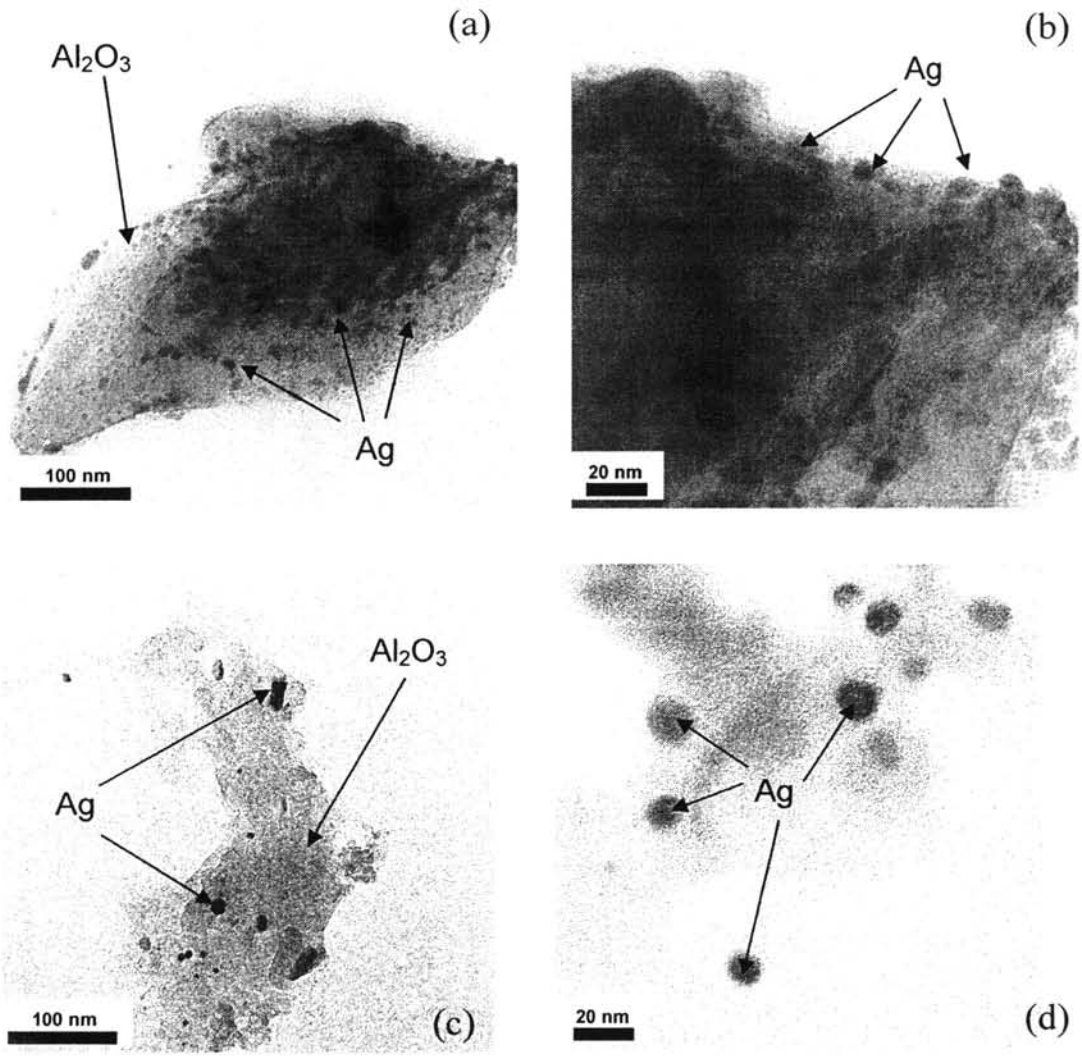

Figure 4.22 TEM images of fresh and spent 12.5 wt% Ag/(LSA)α-Al_2O_3: (a) fresh catalyst at low magnification, (b) fresh catalyst at high magnification, (c) spent catalyst at low magnification, and (d) spent catalyst at high magnification.

Figure 4.22 shows TEM images of spent catalyst as compared to the fresh catalyst. These TEM images suggest that the silver agglomeration occurred after the activity test due to its relatively larger particle size on the spent catalyst. This Ag agglomeration on the surface of the spent catalyst could reasonably contribute to the lower activity.